Title

Thermal Performance of a Conduction-Cooled CCT Dipole ReBCO Magnet: Several Cycles of Cool-Down and Thermal Gradient Measurements

Journal

IEEE Transactions on Applied Superconductivity, 36(3)

ISSN

1051-8223

Authors

Garg, T
Kwon, J
Kovacs, C
et al.

Publication Date

2026-05-01

DOI

10.1109/tasc.2025.3648331

MT29-Sat-Mo-Po.07-03

Thermal Performance of a Conduction-Cooled CCT Dipole ReBCO Magnet: Several Cycles of Cool-Down and Thermal Gradient Measurements

T. Garg[1], J. Kwon[1], C. Kovacs[2], X. Wang[3], M. Majoros[1], M.D. Sumption[1], and E.W. Collings[1]

***Abstract*— This paper presents experimental results from conduction-cooled thermal testing of a ReBCO canted cosine theta (CCT) magnet (C2), originally designed and fabricated at LBNL using CORC® cables. While the performance of the coil under liquid helium and nitrogen environments has been previously established, this study explores its behavior under conduction cooling using a large test cryostat at The Ohio State University. The magnet, measuring 613 mm in length and weighing ~75 kg, consists of four helical layers wound with ReBCO-based CORC® wire and was thermally anchored to a copper cold ring supported by a G-10 strongback. Cooling was provided by two Sumitomo RDK-415D cryocoolers, offering a combined 3 W at 4.2 K and 150 W at 77 K. Multiple thermal cycles were performed, with cooldown durations of up to 45 hours. Final base temperatures of approximately 10.8 K (at the coil edge) and 12.0 K (at the coil center) were achieved, with an axial temperature difference of approximately 1.2 K. The warm-up period extended over approximately 24.6 hours. Voltage measurements from all four layers were recorded during cooldown and warmup. The system demonstrated stable cooldown performance, repeatable gradients, and good thermal anchoring. These results support the feasibility of conduction cooling in large-scale HTS magnets, aligning with broader goals for "green" cryogen-free accelerator technologies and paving the way for more sustainable, scalable, and energy-efficient high-field magnet systems in next-generation particle accelerators.**

***Index Terms*— Canted cosine theta magnets, High-temperature superconductors (HTS), Conduction cooling, and Particle accelerator magnets.**

I. Introduction

HIGH-ENERGY particle accelerators have traditionally relied on high-field superconducting dipole magnets to achieve the strong, stable fields required for beam steering and focusing. Low-temperature superconductors (LTS), notably NbTi and Nb_3Sn, have enabled operational fields in the 6–12 T range in modern accelerators, with state-of-the-art research magnets achieving even higher fields [1], [2], [3], [4]. A major advance in this context has been the canted cosine theta (CCT) geometry, which provides exceptional field quality, training-free behavior, and reduced mechanical stress compared to conventional cos(θ) magnets [5], [6], [7], [8]. Successful demonstrations of LTS-based CCT dipoles include Nb_3Sn magnets exceeding 5 T [5], [6] and large-aperture designs intended for hybrid or insert magnet studies [7], [8]. Despite their success, LTS magnets are fundamentally limited by their reliance on liquid helium, an increasingly scarce and expensive resource that demands extensive infrastructure and high operational costs [2], [4], [9]. The environmental and logistical challenges of helium-based cryogenics have prompted an international shift toward sustainable, energy-efficient "green accelerator" technologies [9], [10].

In response, high-temperature superconductors (HTS), especially ReBCO (rare-earth barium copper oxide) tapes and cables, have emerged as transformative materials, enabling reliable operation at higher temperatures (10–20 K) and in ultra-high magnetic fields [11], [12], [13]. When implemented in the CCT geometry, HTS conductors such as CORC® cables that combine high current density, mechanical resilience, and compatibility with modular accelerator designs are particularly well-suited for next-generation accelerators. [11], [14], [15].

While cryocoolers typically operate at a lower fraction of Carnot efficiency than large helium cryoplants, HTS magnets benefit from higher operating temperatures (e.g., 10–20 K) where the Carnot coefficient of performance is much more favorable. This temperature advantage can, in principle, compensate for lower machine efficiency and allows overall energy consumption for HTS systems to be competitive with traditional LTS approaches.

A critical distinction between HTS and LTS magnets is the operating temperature regime. HTS materials such as CORC cables are designed to operate efficiently at 10-20 K, eliminating the need for 4.2 K operation required by NbTi and Nb_3Sn. Operating an HTS magnet at liquid helium temperature (4.2 K) would negate the fundamental advantage of these materials. This elevated temperature regime offers significant benefits: the Carnot coefficient of performance at 10K is approximately 2.4× more favorable than at 4.2 K, making compact cryocoolers thermodynamically well-matched to HTS requirements without the extensive helium liquefaction

This work was supported in part by the United States Department of Energy, Office of Science, Division of High Energy Physics under Grant DE-SC0011721. *(Corresponding author: T. Garg).*

T. Garg, J. Kwon, M.D. Sumption, M. Majoros, and E.W. Collings are with the Center for Superconducting and Magnetic Materials, Department of Materials Science and Engineering, The Ohio State University, Columbus, OH 43210, USA (e-mail: garg.206@ osu.edu).

C. Kovacs is with Scintillating Solutions LLC., Columbus, OH, USA

X. Wang is with Lawrence Berkeley National Laboratory, Berkeley, CA 94720, USA.

infrastructure needed for LTS systems.

A notable realization of this approach is the four-layer C2 CCT dipole, developed at Lawrence Berkeley National Laboratory, which demonstrated a 2.9 T central field at 4.2 K and forms the basis of the present study [16]. Field quality and magnetization modeling of C2-type ReBCO CCT dipoles have demonstrated that these magnets can achieve accelerator-grade stability and reproducibility [17], and thermal modeling has confirmed robust quench protection and temperature uniformity during cyclic cooling [18]. The C2 magnet design builds on earlier work establishing the feasibility of CORC®-based CCT magnets. [19].

The integration of conduction cooling using compact cryocoolers in place of liquid helium baths is now being explored for HTS-based CCT dipole magnets, eliminating the need for massive cryoplants and enabling decentralized, infrastructure-light accelerator facilities [12], [20], [21]. Recent experiments demonstrate conduction-cooled ReBCO CCT prototypes operating above 10 T, with reliable cyclic cool-down and energization without cryogens [11], [12], [21], [22].

The conduction cooling of superconducting magnets using cryocoolers has been studied extensively in various contexts, including commercial applications such as MRI magnets and smaller research-scale systems [23], [24], [25], [26]. Most of these existing examples involve cooling magnets immersed in a finite liquid helium reservoir or employ minimum liquid helium volumes that serve as heat exchange media. These configurations, while effective, are distinct from true direct conduction cooling, where the entire magnet is cooled via solid conduction paths without reliance on liquid cryogens.

With respect to conduction cooling specifically, a thorough survey of the literature reveals numerous instances of conduction-cooled superconducting solenoids and compact magnets, predominantly using low-temperature superconductors such as NbTi [27], [28] or relatively small-scale high-temperature superconductor (HTS) coils, predominantly YBCO and BSCCO pancake configurations [29], [30]. However, the application of direct conduction cooling to model dipole insert-level HTS cosine-theta dipole magnets designed for accelerator use, particularly those employing advanced cable architectures like ReBCO, remains rare, with few references in this specific area. To our knowledge, no prior work reports a conductor-geometry and magnet-type combination comparable to that presented here: an extended canted-cosine-theta dipole winding geometry, fabricated using ReBCO HTS cable, cooled solely via direct conduction from cryocoolers without liquid helium reservoirs.

This distinction is critical. Unlike compact solenoids or magnets housed in helium baths, the conduction heat must be extracted along the entire axial length of the dipole winding, with the potential to induce significant temperature gradients longitudinally. In addition, the magnet's multilayer winding structure necessitates radial heat transport, further complicating effective conduction cooling. Our manuscript investigates these thermal gradients in an HTS cosine-theta dipole magnet cooled by direct conduction, supported by detailed cross-sectional thermal characterization.

In this study, we focus on thermal characterization of the magnet winding itself, using a generic open-box cryostat to demonstrate that conduction cooling can achieve acceptable temperature gradients along the winding. In practice, a dedicated cryostat for accelerator magnets would be much more compact and tailored, but that is beyond our current scope. Our experimental system focuses on assessing the baseline performance and thermal cycling stability, providing initial feasibility data for future optimization.

Moreover, the experimental approach includes functional thermal cycling of the system, assessing the magnet's superconducting transition temperature (T_c) response and its repeatability across multiple cooldown and warm-up cycles. These cycling studies provide an assessment of potential magnet degradation.

As motivation, we compare cooling efficiencies following Bottura (2024) [31]. System efficiency depends on the Carnot coefficient of performance (COP) and the figure-of-merit (f), representing the fraction of Carnot efficiency achieved. For advanced helium liquefaction plants at 4.2 K, $f \approx 30\%$, while compact cryocoolers at 10-20 K typically have f = 10-15%. Using COP values $COP_{4.2K} \approx 0.014$ and $COP_{20K} \approx 0.071$, the electrical input per watt of cooling, $P_{input} = (COP \times f)^{-1}$, is about 238 W/W at 4.2 K and 118 W/W at 20 K.

Thus, despite lower machine efficiency, the higher operating temperature for HTS systems means that input power per cooling watt should be competitive or even favorable compared to liquid helium-based designs. This supports the technical viability of cryocooler-based "green accelerator" magnets, especially as HTS conductors can sustain high fields and performance well above 4.2 K.

This paper presents the first systematic thermal characterization of a four-layer, conduction-cooled CORC-based CCT dipole magnet tested at The Ohio State University. The focus is on thermal performance: cooldown behavior, longitudinal and radial temperature gradients across the 613 mm-long multilayer structure, and thermal cycling stability.

II. Experimental

A. Magnet Description

The magnet under test is a four-layer C2 canted cosine theta (CCT) dipole originally developed at Lawrence Berkeley National Laboratory (LBNL) and described in detail by Wang et al. [16]. Each layer is wound with 30-tape CORC® cable manufactured by Advanced Conductor Technologies, using 2 mm wide ReBCO tapes from SuperPower Inc. The cables are helically wound onto aluminum bronze mandrels with half-depth radial grooves to form the CCT architecture. The inner diameter of the magnet is 65 mm, the outer diameter is 127 mm, and the total magnetic length is 613 mm. Including current leads, the full assembly length is approximately 1.5 m, matching the spatial constraints of the Ohio State Large Cryostat (OLC). The total coil mass is approximately 75 kg.

To monitor the thermal behavior of the magnet during operation, three Cernox™ temperature sensors were mounted at evenly spaced positions along the outermost layer of the coil. These sensors were used to measure temperature gradients across the coil surface during cooldown and steady-state operation in the OLC.

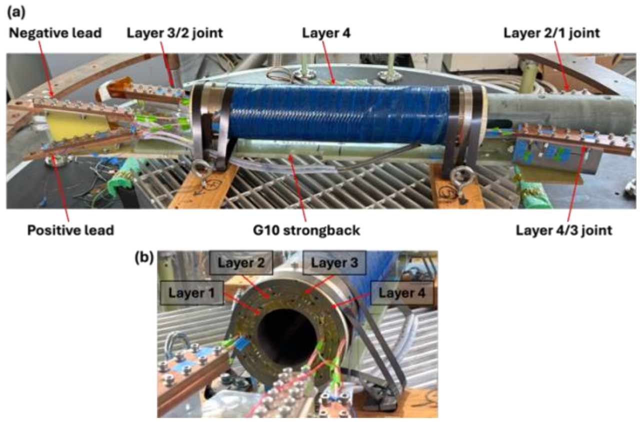

Fig. 1. C2 dipole magnet, (a) highlighting the CORC® winding layers, Nb-Ti current leads, interlayer joints, and the G-10 structural base used for cryostat integration, (b) cross-section view representing all the layers of the dipole magnet.

TABLE I
COIL SPECIFICATIONS

Physical Parameters	**Specification**
Number of CCT layers	4
ID (inner most layer), mm	65
OD (outer most layer), mm	127 mm
Number of turns in each layer	40
Total length of cable in 4 layers, m	69.3 m
Mandrel length, mm	613 mm
Mandrel material	aluminum bronze 954
Magnet mass, kg	~75 kg
I_{op} (77 K), A	300 A
I_{op} (4.2 K), A	5000 A

B. Conduction Cooling and Cryostat Assembly

The magnet was tested in a horizontal setup inside the OLC, employing conduction cooling via two Sumitomo RDK-415D pulse tube cryocoolers. These cryocoolers provide a combined cooling power of approximately 3 W at 4.2 K and 150 W at 77 K.

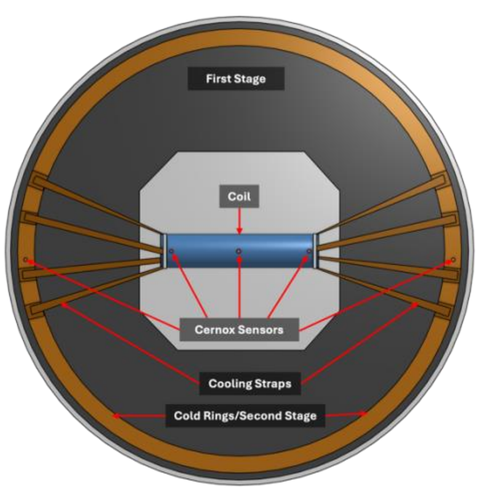

Fig. 2. Schematic showing the cooling arrangement of the coil and sensor placement in the OLC.

The coil was mechanically supported by a G-10 strongback, which rested on an aluminum support thermally anchored to the first stage of the cryocooler. A system of high-conductivity copper straps was bolted to the end flanges of the coil to thermally link it to the cold ring (schematic representation in Figure 2).

To minimize radiative loading, the entire coil was wrapped in multiple layers of aluminized Mylar (MLI) insulation (Figure 3b) and enclosed within a thermal shield coupled to the first stage of the cryocooler. The cryostat incorporates a cold ring and cryocoolers within its vacuum-insulated stainless-steel chamber, along with thermally anchored radiation shield supports. The magnet and current leads remained on the G-10 strongback during cooldown.

TABLE II
CRYOSTAT SPECIFICATIONS

Component	**Specification**
Cryocoolers	2 × Sumitomo RDK-415D
Cooling Power	3 W @ 4.2 K, 150 W @ 77 K (combined)
Cold Ring	OFHC Copper
Supports	G-10 Strongback
Anchoring	Copper straps to coil end flanges
Radiation Shield	MLI + first-stage thermal shield
Current Leads	HTS flexible leads

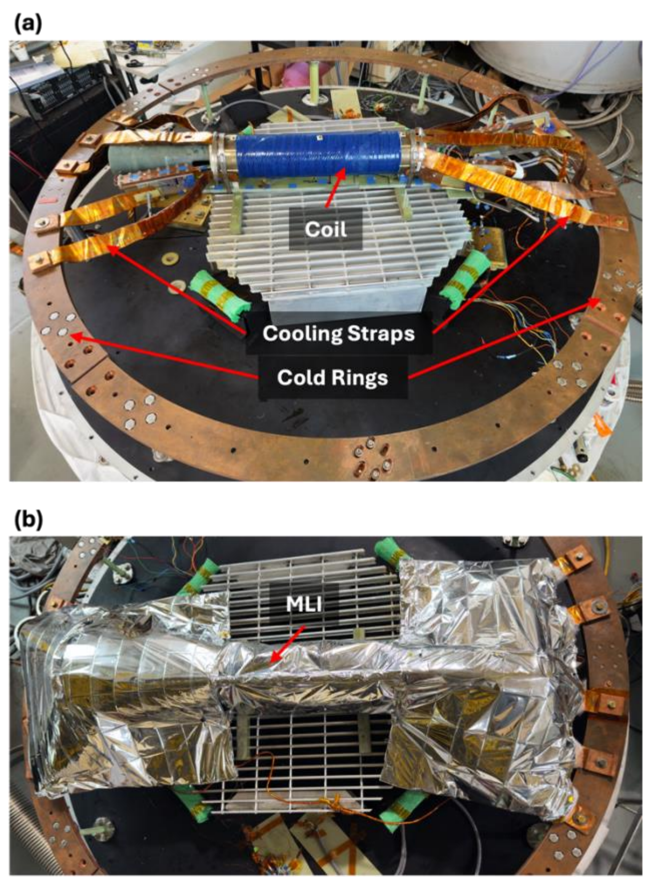

Fig. 3. Assembly of the C2 ReBCO dipole magnet inside the conduction-cooled OLC. (a) Exposed coil showing copper thermal connections and structural supports. (b) Magnet after MLI wrapping and thermal shielding installation.

C. Measurement Procedure

Temperature monitoring was performed using Cernox™ sensors attached to the outer surfaces of each coil layer with GE varnish to ensure strong thermal coupling. Additional sensors were installed at the cold ring. All temperature signals were routed to a Lakeshore 336 temperature controller and logged at 300-second intervals via a LabVIEW-based data acquisition system. Voltage taps were soldered to the terminations of each winding layer, allowing the measurement of both total magnet voltage and individual layer voltages.

During the experiment, the system was evacuated using rotary and turbomolecular pumps. The magnet was cooled from room temperature to cryogenic base temperature under continuous monitoring of all temperature and voltage channels. A bias current of 0.5 A was applied continuously during thermal cycling to monitor superconducting transition temperatures. This current level was chosen to provide a sufficient voltage signal for accurate T_c determination while minimizing self-heating effects. The warm-up process was initiated by powering down the cryocoolers, with continued data acquisition throughout to capture thermal recovery and any voltage evolution.

All sensors were calibrated prior to testing, with total uncertainty in temperature measurement estimated below 0.2 K. Data were analyzed to determine thermal gradients, time constants, and the stability of electrical joints during thermal cycles and current injection.

The primary objective of this work was the thermal characterization of the conduction cooling system. Specifically, we aimed to: (1) demonstrate that a 75 kg HTS CCT dipole magnet can be cooled to ~10 K via direct conduction without liquid helium, (2) characterize longitudinal temperature gradients, and (3) assess thermal stability over multiple cycles.

III. Results and Discussion

A. Cooldown and Warm-Up Behavior

The conduction-cooled C2 magnet underwent multiple thermal cycles using a two-stage cryocooler system in the OLC. Cooldown from room temperature to base temperature took approximately 45 hours, with the cold head reaching a minimum of 9.2 K and the coil sensors stabilizing at 10.8 K (Sensor-A) and 12.0 K (Sensor-C). The axial temperature gradient of ~1.2 K observed across Sensor-A, Sensor-B, and Sensor-C (mounted on Layer 4 at the lead, midpoint, and return ends, respectively) remained consistent across cooldown cycles, indicating reliable thermal anchoring and repeatability. Coldhead-1 and Coldhead-2 showed steady temperature progression throughout the cycle, confirming cryocooler functionality.

Following the cooldown, a warm-up was initiated without active heating. Over 24.6 hours, the coil temperature rose gradually to approximately 122 K. All three sensors exhibited smooth, monotonic increases, consistent with uniform thermal coupling between the coil body, copper support structure, and cryostat radiation environment. Cold-head sensors reflected matching trends, further validating system stability.

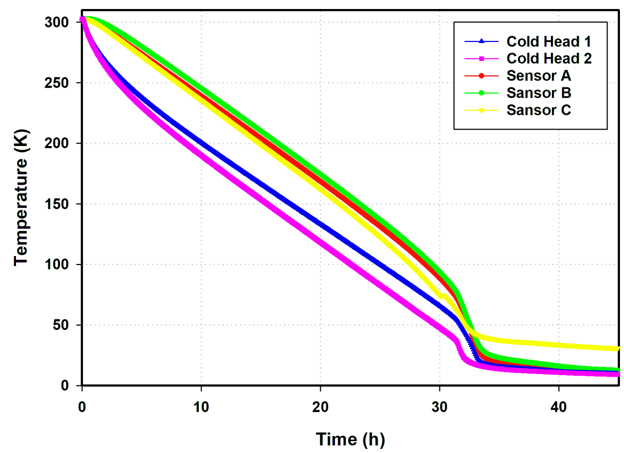

Fig. 4. Temperature profile of the C2 coil during cooldown. Sensors mounted along Layer 4 (Sensor-A, Sensor-B, Sensor-C) recorded a stable axial gradient from ~12.0 K to ~10.8 K over 45 hours. Coldhead-1 and Coldhead-2 data are included for thermal reference.

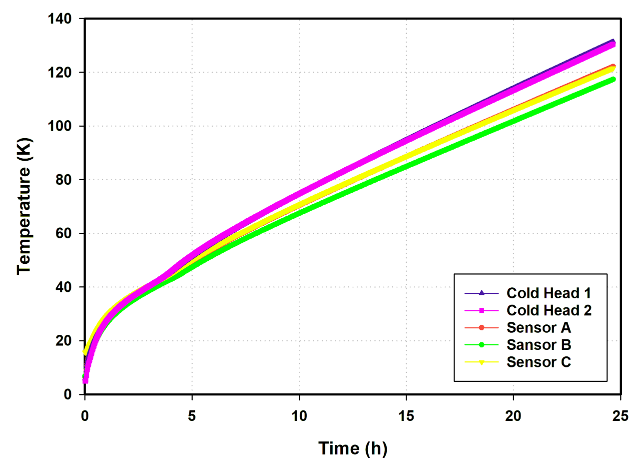

Fig. 5. Warm-up temperature evolution recorded by Sensor-A, Sensor-B, and Sensor-C. The coil warmed to ~122 K uniformly across the axial length within 24.6 hours. Coldhead data indicate a consistent system response.

B. Voltage Behavior During Thermal Transitions

Voltage measurements were continuously recorded across all four CORC® layers throughout cooldown and warm-up. During cooldown, voltages steadily declined as the temperature decreased, with all layers showing clean superconducting transitions and with no evidence of discontinuities. This indicates stable and effective thermal conduction throughout the cable architecture.

During warm-up, the voltage increased gradually as each layer passed through its critical temperature. The transitions were consistent across all four layers, confirming the accuracy of the voltage instrumentation and the integrity of all four voltage taps. The current used during these voltage measurements was 0.5 A.

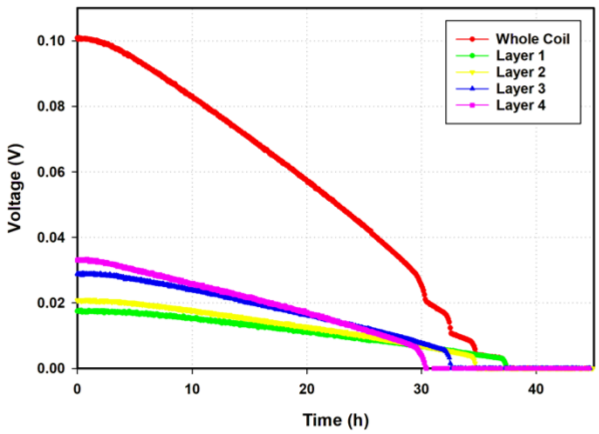

Fig. 6. Voltage behavior during cooldown at 0.5 A bias current. All four CORC® layers showed clean superconducting transitions without instabilities. Sensor-based temperature correlation confirms voltage response.

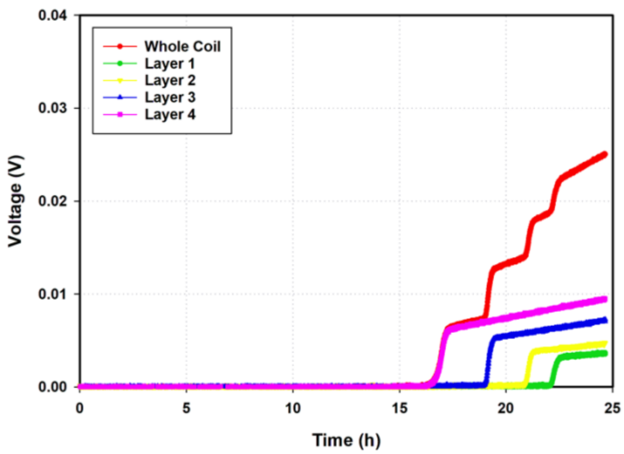

Fig. 7. Voltage response during warm-up at 0.5 A bias current. All layers, including Layer 4, exhibited resistive transitions aligned with rising temperatures measured by Sensor-A, B, and C.

A clear sequential superconducting transition was observed from Layer 4 (outermost) to Layer 1 (innermost), which aligns well with previous observations during the vertical test [16]. This sequential behavior highlights the effectiveness and consistency of the thermal conduction path established in the coil structure.

C. Several Cooldown Cycles and T_c Characterization

The multi-cycle cooldown experiments demonstrate consistent and reliable operation of the cold head and coil temperature control. The magnet was cooled several times to the target temperature of approximately 10 K, requiring about 45 hours to reach this base temperature with a maximum temperature difference of 1.2 K along its length. Across three cycles, all monitored points showed repeatable thermal profiles with minor cycle-to-cycle differences due to typical variations in thermal load or heat exchange (Figure 1).

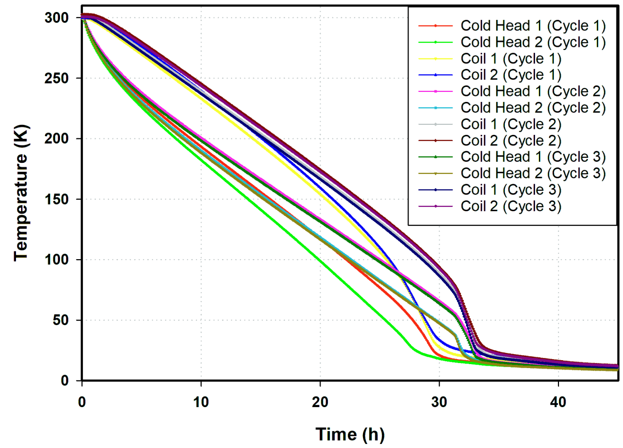

Fig. 8. Cooldown temperature of coils and cold heads over three cycles, demonstrating repeatable and stable cooling.

Superconducting transition temperature (T_c) determination was carried out by tracking coil voltage as a function of temperature during each cycle. Sharp voltage rises marking the onset of resistivity were observed near ~90–100 K, with both cycles exhibiting consistent T_c values and transition sharpness (Figure 9).

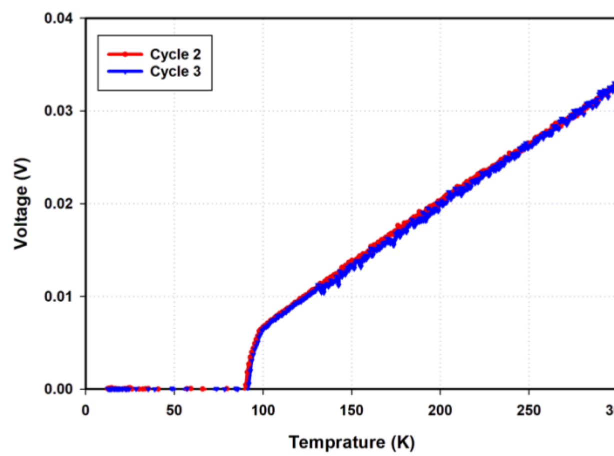

Fig. 9. Voltage versus temperature for cycles 2 and 3, indicating consistent superconducting transitions (T_c) for the coil.

IV. Conclusion

This study presents the initial conduction-cooled evaluation of the C2 ReBCO canted cosine theta (CCT) dipole magnet, originally designed for liquid cryogen immersion. Through multi-day cooldown and warm-up cycles, we observed a consistent axial temperature difference of ~1.2 K and base temperatures below 12 K. Voltage traces from all four CORC® layers demonstrated clean superconducting transitions during cooldown and well-behaved resistive onsets during warm-up with a bias current of 0.5 A, with no signs of instability. These results demonstrate effective mechanical and thermal contact between the coil and conduction-cooled hardware, and indicate that stable, low-power operation may be achievable without reliance on large cryogen volumes. While the injected current levels were modest, they serve as an encouraging baseline for future, higher-power conduction-cooled testing. Overall, this work supports the transition toward cryogen-free, compact, and energy-efficient superconducting magnet systems. It provides an early but important step toward realizing HTS-based magnets for accelerator and fusion applications that align with emerging green technology goals.

In summary, the novelty of this work lies in the application of direct conduction cooling to a model insert-scale HTS canted-cosine-theta dipole magnet of accelerator relevance, the detailed characterization of axial and radial temperature gradients within a complex winding structure, and the exploration of magnet behavior under thermal cycling at elevated base temperatures. These aspects collectively represent a significant advancement beyond existing conduction-cooled superconducting magnet literature.

References

[1] L. Bottura, G. de Rijk, L. Rossi, and E. Todesco, "Advanced Accelerator Magnets for Upgrading the LHC," *IEEE Trans. Appl. Supercond.*, vol. 22, no. 3, pp. 4002008–4002008, Jun. 2012, doi: 10.1109/TASC.2012.2186109.

[2] D. Arbelaez *et al.*, "Training-free demonstration of a 5.4 T Nb_3Sn Canted–Cosine–Theta accelerator dipole impregnated with paraffin wax," *Supercond. Sci. Technol.*, vol. 37, no. 6, p. 065015, May 2024, doi: 10.1088/1361-6668/ad44e6.

[3] D. Arbelaez *et al.*, "Status of the Nb_3Sn Canted-Cosine-Theta Dipole Magnet Program at Lawrence Berkeley National Laboratory," *IEEE Trans. Appl. Supercond.*, vol. 32, no. 6, pp. 1–7, Sep. 2022, doi: 10.1109/TASC.2022.3155505.

[4] L. Brouwer, M. Juchno, D. Arbelaez, P. Ferracin, and G. Vallone, "Design of CCT6: A Large Aperture, Nb_3Sn Dipole Magnet for HTS Insert Testing," *IEEE Trans. Appl. Supercond.*, vol. 32, no. 6, pp. 1–5, Sep. 2022, doi: 10.1109/TASC.2022.3151723.

[5] S. Caspi *et al.*, "Canted–Cosine–Theta Magnet (CCT)—A Concept for High Field Accelerator Magnets," *IEEE Trans. Appl. Supercond.*, vol. 24, no. 3, pp. 1–4, Jun. 2014, doi: 10.1109/TASC.2013.2284722.

[6] P. Ferracin *et al.*, "Towards 20 T Hybrid Accelerator Dipole Magnets," *IEEE Trans. Appl. Supercond.*, vol. 32, no. 6, pp. 1–6, Sep. 2022, doi: 10.1109/TASC.2022.3152715.

[7] L. Bottura and B. Bordini, "HTS Potential and Needs for Future Accelerator Magnets," Apr. 01, 2025, *arXiv*: arXiv:2503.23048. doi: 10.48550/arXiv.2503.23048.

[8] V. S. Kashikhin *et al.*, "Development and test of single-layer common coil dipole wound with reacted Nb_3Sn cable," *IEEE Trans. Appl. Supercond.*, vol. 14, no. 2, pp. 353–356, Jun. 2004, doi: 10.1109/Tasc.2004.829128.

[9] L. Liu *et al.*, "Mechanical Analysis and Testing of Conduction-Cooled Superconducting Magnet for Levitation Force Measurement Application," *Crystals*, vol. 13, no. 7, Jul. 2023, doi: 10.3390/cryst13071117.

[10] D. Zhang *et al.*, "Instrumentation, cooling, and initial testing of a large, conduction-cooled, react-and-wind MgB_2 coil segment for MRI applications," *Supercond. Sci. Technol.*, vol. 31, no. 8, p. 085013, Jul. 2018, doi: 10.1088/1361-6668/aacae3.

[11] X. Wang *et al.*, "A 1.2 T canted cosθ dipole magnet using high-temperature superconducting CORC® wires," *Supercond. Sci. Technol.*, vol. 32, no. 7, p. 075002, May 2019, doi: 10.1088/1361-6668/ab0eba.

[12] K. Kim *et al.*, "Design and Performance Estimation of a 20 T 46 mm No-Insulation all-REBCO User Magnet," *IEEE Trans. Appl. Supercond.*, vol. PP, pp. 1–1, Feb. 2020, doi: 10.1109/TASC.2020.2975166.

[13] X. Wang, U. P. Trociewitz, and J. Schwartz, "Critical current degradation of short $YBa_2Cu_3O_{7-\delta}$ coated conductor due to an unprotected quench," *Supercond. Sci. Technol.*, vol. 24, no. 3, p. 035006, Dec. 2010, doi: 10.1088/0953-2048/24/3/035006.

[14] C. Kovacs, M. Majoros, M. D. Sumption, and E. W. Collings, "Magnetization Measurements of CORCTM and Roebel Type YBCO Cables for Accelerators Using a ±3-T Dipole Magnetometer," *IEEE Trans. Appl. Supercond.*, vol. 29, no. 5, pp. 1–5, Aug. 2019, doi: 10.1109/TASC.2019.2898254.

[15] T. Garg, J. Jaroszynski, E. S. Choi, M. D. Sumption, M. Majoros, and E. W. Collings, "Magnetization in ReBCO-Based CORC Cables in Magnetic Fields up to 30 T for Accelerator Applications," *IEEE Trans. Appl. Supercond.*, vol. 35, no. 5, pp. 1–5, Aug. 2025, doi: 10.1109/TASC.2025.3540991.

[16] X. Wang *et al.*, "Development and performance of a 2.9 Tesla dipole magnet using high-temperature superconducting CORC® wires," *Supercond. Sci. Technol.*, vol. 34, no. 1, p. 015012, Dec. 2020, doi: 10.1088/1361-6668/abc2a5.

[17] M. Majoros, M. D. Sumption, C. S. Myers, and E. W. Collings, "Canted Cosine Theta Dipole Magnet Wound Using REBCO CORC Cables–The Effect of Magnetization on Magnetic Field Quality," *IEEE Trans. Appl. Supercond.*, vol. 33, no. 5, pp. 1–5, Aug. 2023, doi: 10.1109/TASC.2023.3265574.

[18] M. Majoros, M. D. Sumption, and E. Collings, "Thermal Modeling of Canted Cosine Theta Dipole Magnets wound using Defected REBCO Cables," *IEEE Trans. Appl. Supercond.*, vol. 35, no. 5, pp. 1–5, Aug. 2025, doi: 10.1109/TASC.2024.3524983.

[19] X. Wang *et al.*, "A viable dipole magnet concept with REBCO CORC® wires and further development needs for high-field magnet applications," *Supercond. Sci. Technol.*, vol. 31, no. 4, p. 045007, Mar. 2018, doi: 10.1088/1361-6668/aaad8f.

[20] M. Majoros, M. D. Sumption, S. Xue, C. S. Myers, and E. W. Collings, "A Field Quality Modeling in Canted Cosine Theta Dipole Magnets Wound Using REBCO Cables," *IEEE Trans. Appl. Supercond.*, vol. 34, no. 5, pp. 1–4, Aug. 2024, doi: 10.1109/TASC.2024.3365092.

[21] D. M. Araujo *et al.*, "Preliminary Integration for Testing HTS Feather-M2 in the FRESCA2 Dipole Magnet," *IEEE Trans. Appl. Supercond.*, vol. 30, no. 4, pp. 1–5, Jun. 2020, doi: 10.1109/TASC.2020.2979393.

[22] S. Hu *et al.*, "Design and Construction of a 20-T 30-mm All HTS Conduction-Cooled User Magnet," *IEEE Trans. Appl. Supercond.*, vol. 34, no. 3, pp. 1–5, May 2024, doi: 10.1109/TASC.2024.3356430.

[23] H. Qu et al., "Thermal Analysis of the 4 K Cryostat Within a 1.5 T Conduction-Cooled Superconducting Magnet for Whole-Body MRI Application," *IEEE Trans. Appl. Supercond.*, vol. 34, no. 8, pp. 1–5, Nov. 2024, doi: 10.1109/TASC.2024.3420212.

[24] Z. Xu et al., "Design and simulation of a 7.0 T conduction cooled superconducting magnet," *Sci Rep*, vol. 15, no. 1, p. 15699, May 2025, doi: 10.1038/s41598-025-00643-w.

[25] H. Xie, S. Chen, W. Sun, and Q. Wang, "Development of a 3 T Conduction-Cooled Animal MRI Superconducting Magnet With a 300 mm Warm Bore," *IEEE Trans. Appl. Supercond.*, vol. 34, no. 8, pp. 1–5, Nov. 2024, doi: 10.1109/TASC.2024.3420331.

[26] Y. Wang et al., "Cryogen-free superconducting magnetic resonance imaging system: A review," *Fundamental Research*, May 2025, doi: 10.1016/j.fmre.2025.05.006.

[27] Y. Dai, L. Yan, B. Zhao, S. Song, Y. Lei, and Q. Wang, "Tests on a 6 T Conduction-Cooled Superconducting Magnet," *IEEE Trans. Appl. Supercond.*, vol. 16, no. 2, pp. 961–964, June 2006, doi: 10.1109/TASC.2006.873331.

[28] S. Kar et al., "Analysis of thermal stability of conduction-cooled LTS magnet," *Cryogenics,* vol. 52, no. 12, pp. 739–743, Dec. 2012, doi: 10.1016/j.cryogenics.2012.06.003.

[29] Y. Kim, S. Hahn, J. Voccio, J. Song, J. Bascuñán, and Y. Iwasa, "Strain in YBCO Double-Pancake Coil With Stainless Steel Overband Under External Magnetic Field," *IEEE Trans. Appl. Supercond.*, vol. 25, no. 3, pp. 1–4, June 2015, doi: 10.1109/TASC.2014.2365738.

[30] Y. Chen et al., "Improving the thermodynamic performance of small-scale HTS cooling system based on the temperature-distributed method in regenerative refrigerators," *Energy,* p. 138758, Oct. 2025, doi: 10.1016/j.energy.2025.138758.

[31] L. Bottura, "III.16 — Magnets for future colliders: the Muon Collider as a case study," *CERN Yellow Reports: School Proceedings*, vol. 3, no. I–IV, pp. 2179–2179, Nov. 2024, doi: 10.23730/CYRSP-2024-003.2179.